Journal of Mechanical Science and Technology, Volume 37, Issue 6, June 2023, pp. 3185 - 3195
DOI: 10.1007/s12206-023-0542-2

The Effect of Multiple Pairs of Vortex Generators on the Thermal Performance of Plate Fin Heat Sink

Mani Sekaran Santhanakrishnan

Cranfield, Bedfordshire, United Kingdom

(Received 000 0, 2020; Revised 000 0, 2020; Accepted 000 0, 2020) -please leave blank

Keywords: Plate Fin Heat Sink; Vortex Generators; Heat Exchangers; Response Surface Model

Correspondence to:. Mani Santhanakrishnan / manisekaran.san@gmail.com

Abstract In this study heat transfer characteristics of multiple pairs of vortex generators (VG) mounted on the vertical plate fins of plate fin heat sink are evaluated using computational fluid dynamic simulations. The delta winglet pairs are used as longitudinal vortex generators, and they are mounted one after the other in the axial direction. Critical design parameters for the double pair of vortex generators are identified and a design of experiment-based simulations are carried out to develop a response surface model for Nusselt number and thermal hydraulic performance parameter. The study results have shown that the winglet length is a critical design parameter than the winglet height and the axial inter-VG distance between VG pairs plays a crucial role in improving the heat transfer characteristics. The optimum inter-VG distance for a double pair of VG is evaluated and it is 2.2 to 3 times the length of the delta-winglet. Thermal hydraulic performance of plate fin heat sink with double pair of VG is 1.49 times higher than the plain plate fin heat sink. Finally, the variation of heat transfer characteristics against velocity is also evaluated for the plate fin heat sink with a double pair of VG.

1. Introduction

Power density levels of microelectronic components have tremendously increased in the recent years. This calls for effective cooling technology for their normal operation and long life. Plate fin heat sinks (PFHS) are widely used for microelectronics thermal management. PFHS typically have several thin plate fins kept along the flow direction. Dimples, roughness, ribs and vortex generators are used to increase the cooling effectiveness of plate fin heat sink. Out of these, use of vortex generator which produces longitudinal vortices inside the heat sink channel has given promising results.

The vortex generators (VG) have been used for long time to increase the heat transfer and to suppress the flow separation. Fiebeg et al. [1] studied the thermal performance of longitudinal VG on a rectangular channel experimentally in 1991. The results showed that local heat transfer was increased by 200% and Colburn factor was increased from 20 to 60%. They have considered different VG like delta winglet pair and rectangular winglet pair, which were punched from the bottom flat plate. Highest heat transfer enhancement was reported by delta wings, followed by delta winglets and rectangular winglets. The vortex strength per unit VG generated by delta wing is larger than that of a rectangular wing because of the longer side edges of delta wing for the same wing area and span. Furthermore, the transverse distance between the LV axes is less for delta wings than for rectangular wings of the same span. This results in a higher peak and higher heat transfer performance by the delta wing VG.

Most of the VG research for heat transfer enhancement was conducted on fin and tube heat exchangers. Pesteei et al. [2] experimentally found that the best location for winglet type VG on fin and tube heat exchanger, is at 50% of the tube diameter in both streamwise and spanwise direction. Wu and Tao [3], numerically studied the longitudinal VG on a laminar rectangular channel and found that Nusselt number (Nu) decreases as the VG is moved away from the inlet, and as the transverse distance between the VG pair is decreased. Increasing the length of VG will enhance heat transfer more than increasing the height, without significantly impacting on the flow loss.

Yang, Jhong et al. [4] examined the air side performance of heat sinks with fins having patterns like delta shape VG, semi-circular VG, plain fin and their combinations. The study found that, semi-circular VG are effective at developing flow region. For the same pumping power and same heat transfer capacity, it was found that asymmetric design of VG fin with plain fin produced best result. Effect of the longitudinal VG on the heat transfer of both the surfaces (upper side and lower side) of one fin in a fin-and-tube heat exchanger was studied by Wu and Tao [5]. VG is a pair of delta winglet punched at angles ranging from 15° to 60°. The study showed that the heat transfer increases with Reynolds number (Re) and attack angle.

If the vortex generating winglets are arranged in such a way that the spanwise distance between leading edges are much higher than spanwise distance between trailing

Published by Springer. This is the Author Accepted Manuscript.
The final published version (version of record) is available online at DOI:10.1007/s12206-023-0542-2. Please refer to any applicable publisher terms of use.

edges then this arrangement is called Common-flow-up (CFU). On the other hand if, the distance between trailing edges are higher than distance between the leading edges then it is called common-flow-down (CFDN) arrangement.

Li et al. [6] studied the effect of externally mounted delta winglet VG on the performance of PFHS and found that the attack angle of 30° is preferable. VG effect is better at lower Re numbers and CFU is beneficial than CFDN configuration. Later, Li et al. [7], investigated the effect of delta wing VG mounted upstream to the PFHS.

References [8] and [9] did 3 dimensional CFD studies on fin and tube heat exchanger with rectangular plate VG. Former studied the mechanism of heat transfer enhancement due to VG and found that mounting the VG in staggered arrangement will have less pressure drop requirement than the inline arrangement. Reference [9] studied inline tube arrangement against staggered tube arrangement and found that VG performance is higher in inline tube arrangement than in the staggered tube arrangement.

Sinha et al. [10] studied the effect of different orientation of two rows of winglet arrays on a plate fin heat exchanger. The results showed that CFU followed by CFU rows of VG have performed better than other configurations. Zhou [11] investigated plane and curved winglets with punched holes. He found that curved VGs are better than plain VGs and the holes on the VG improve the thermo-hydraulic performance (THP).

Aliabadi et al. [12] evaluated the effect of rectangular wing type transverse VG on a plate fin heat exchanger channel using 3D CFD. Based on the study results, correlations for Nu were derived. The results also showed that the wing height and wing attack angle were influential parameters than other parameters. Performance of different delta winglet VG inserts in a circular tube was experimentally studied by Aliabadi et al.[13] using water as the working fluid. They have studied 14 different VG configurations and found that maximum performance evaluation criterion of 1.41 is obtained for the best VG configuration.

Reference [14][15] maximize the heat transfer in rectangular channel based on geometric variables of VG using neural network and genetic algorithm. Apart from rectangular channels, VGs were also studied on triangular channels [16] and [17]. The later work numerically evaluated the thermohydraulic performance of triangular fin heat exchanger with multiple delta-winglet type VGs mounted in the streamwise direction. VGs are arranged in CFU and CFDN arrangements. From their study they identified that the optimum distance between the VG pairs (d/Lw) is 0.5, where Lw is the length of the VG.

Ahmed [18] evaluated the effect of fixing ribs in PFHS in comparison to plain PFHS. Different geometric parameters of ribs were studied, namely, different rib size, locations and numbers. They also investigated how many fins can be reduced (material reduction) due to the performance improvement of the VG ribs. Liu et al. [19] numerically and experimentally studied 4 different VGs mounted on the bottom wall of rectangular channel. Results showed that VGs increased the Nu up to 92% when compared with plain channels. Song et al.[20] studied the effect of convexity and concavity on the triangular VGs mounted on the bottom wall for laminar flows. They have also obtained correlation equations for Nu in terms of Re, central angle and other parameters.

Naik and Tiwari [21] studied the location effect of rectangular winglet pair VG on fin and tube heat exchanger. VG attack angle from 15° to 60° were studied. Their study identified the location of VG which will give maximum thermo-hydraulic performance. Naik et al. [22] also studied the characteristics of curved rectangular winglet placed in a channel. They explored the heat transfer enhancement using secondary flow intensity and field synergy principle. Awais and Bhuiyan [23] studied VG to enhance the heat transfer on fin and tube heat exchanger with various tube shapes (circular, oval and rectangular). The optimum attack angle of VG is found to be 165°. It was also found that staggered tube arrangement is better than inline arrangement and oval and circular tubes are better than rectangular tubes. Ahmed et al.[24] and Zheng et al. [25] reviewed the heat transfer augmentation using VG considering both the approaches and applications. For other novel methods to enhance the heat transfer of heat exchangers readers may refer to [26][27].

Among the literatures which studied the PFHS with VG, reference [18] studied ribs mounted on the bottom of the heat sink channel and [28] studied the effect of single pair of VG mounted on the bottom plate and vertical plate of PFHS. The results have shown that the secondary flow generated by VG becomes in-effective after some downstream distance. Hence this study, for the first time, focuses on mounting multiple pairs of VG on the heat sink channel, one after another, to maintain high level of secondary flow throughout the channel length. Further, the ideal inter-VG distance required for better performance is also evaluated and a response surface model for Nu and THP of PFHS is also generated to enable the heat sink designer to work out the first-cut designs.

In this study, the effect of single pair of delta winglet VG and multiple pairs of delta winglet VG mounted on the vertical plate fin are evaluated. Based on the results, double pair of VGs are chosen to study the effect of various design parameters of VG pairs. Further the effect of inter-VG distance on the performance of PFHS and the variation of PFHS with VG performance relative to flow velocity are also evaluated. In this article, section 2 details about the problem description and section 3 describes about the numerical simulation details. Section 4 contains results and discussion. Conclusions are given in Section 5.

2. Problem Description

2.1 Plate Fin Heat Sink

The PFHS are commonly used in the electronic industry

to cool micro electronic devices (Fig.1). Due to rapid miniaturization of electronic devices and continuous increase in power density rating, there is a strong need to increase the effectiveness of PFHS. As the cold fluid gets heated up while flowing through the channel, the cooling effectiveness of the PFHS is quite low at the rear portion of the plate fins. Many different concepts for improving the cooling effectiveness have been investigated in the past, with VG being one of the most promising options. Longitudinal VG create streamwise vortices in the downstream flow, enhancing the thermal mixing and increasing downstream heat transfer. The length to width ratio of the heat sink channels typically range from 10 to 15. The dimensions of the PFHS considered in this study (Fig.1) are given in Table 1.

Parameter	Value (m)
Length of plate fin (L_f)	0.051
Height of the base (H_b)	0.003
Plate fin thickness (δ)	0.0015
Height of the fin (H_f)	0.010
Channel width (W_c)	0.005

Table 1. Geometric details of PFHS.

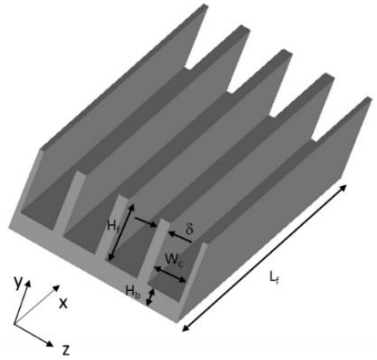


Fig. 1.Plate fin heat sink geometry

2.2 Vortex Generators

Mounting the VG inside the PFHS channel increases the heat transfer, but this comes at the cost of additional drag or higher pumping power requirement. Based on its shape, VGs are classified into three types, namely, i) rectangular wing VG, ii) delta wing VG, and iii) delta winglet pair VG. In this study, delta winglet pair VG arranged in CFDN configuration are considered, as they were found to give better performance than others [5][28]. For the PFHS, the VG can be mounted either on the bottom plate or on the vertical plate fins. The longitudinal vortices emanating from bottom VG will not travel to the whole height of the fins, hence they are not as effective as vertical plate VG [28]. Hence, in this study, the performance of the VG mounted on vertical plate fin are evaluated. The vortices created by the VGs are effective in improving the thermal mixing and heat transfer only for certain downstream distance. Hence multiple pairs of VG can be fixed on the vertical fins, one after the other in the axial direction, to get additional benefits. So, in this study, performance of PFHS with single pair of VG (SPVG) is compared against double pair of VG (DPVG) and triple pair of VG (TPVG) mounted in CFDN arrangement. Study conducted in [28] has shown that higher angle of attack of SPVG yield higher THP performance. Different design variables of delta winglet pair VGs are given below (Fig.2).

Attack angle (β)
Height of VG (H)
Length of VG (L)
Axial distance between consecutive VG pairs (Δx)
Vertical gap between the winglet pair (g)

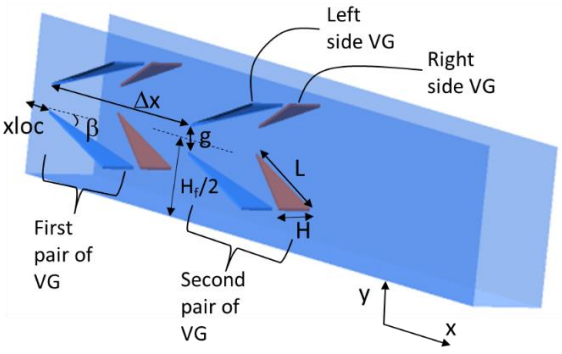


Fig. 2.Plate fin heat sink with double pair of VG on vertical plate fin

3. Numerical Simulation Details

Jonsson and Moshfegh [29] conducted experiments on various plate-fin heat sinks at velocities 8, 10 and 12m/s. All of these heat sinks were fully shrouded, and the top surface is insulated. Later Zhou and Catton [30] investigated the thermal and hydraulic performance of 20 different heat sinks using 3D CFD. It should be noted that the computational results of reference [30] were validated based on the experimental results of [29]. The PFHS geometry and computational domain used in this study are maintained as same as that of [29] to enable the computational results to be compared against the results of [29].

3.1 CFD model

The three-dimensional numerical evaluations are planned to be carried out at velocities 8 to 12m/s. So flow is assumed incompressible and steady. Reynolds numbers corresponding to this range of velocity, based on the pitch of heat sink is 2739 to 4108. Laminar to turbulent transition Re for rectangular channel of aspect ratio 2 is 1900. So, the flow in the heat sink channel is assumed turbulent in nature. Hence in this study, Reynolds Averaged Navier Stokes equations are solved with k-ω SST turbulence model. The mass, momentum and energy equations are shown in Eq. (1-3), where 'u' is mean velocity vector and μ_t is

turbulent dynamic viscosity which is solved by solving k-ω equations. This two-equation turbulence model is developed by Menter [31] and here 'k' represents the turbulent kinetic energy and 'ω' represents the specific dissipation. This model has k-ω formulation at near walls and k-ε formulation at the core flow region. So this model can be used as a low-Reynolds number turbulence model without any extra damping functions and can handle core flow which is sensitive to free-stream turbulence. This model is particularly good for adverse pressure gradient flows and separating flows. Radiation heat transfer is not considered in this study as the focus of this study is to enhance the convective heat transfer due to vortex generators. Further, the magnitude of radiative heat transfer is very less compared to convective heat transfer magnitude. Commercial CFD solver Fluent 18.2 is used to solve the flow physics. Second order upwind differencing scheme has been used, with the SIMPLE algorithm coupling pressures and velocities in a manner that ensures continuity.

The working fluid is considered to be air at an inlet temperature of 293.1K while the PFHS is considered to be formed from Aluminum. Since this work is an extension of [28], material properties of air and aluminum are referred from reference [28]. Heating power value of 10W is considered and the conjugate heat transfer simulation is carried out by simultaneously solving for the heat transfer in the fluid domain (Eq. 1-3) and in the solid domain (Eq. (4)). The symbol for fluid and solid thermal conductivities are k and ks and Pr_t indicates the turbulent Prandtl number of the fluid. (k=0.0242W/m-k, ks=202.4W/m-k) The Eq. 4 is solved in solid regions to compute the temperature and the symbol Q indicates the volumetric heat source in solid region, which is zero in the present study.

$$\nabla.(\rho u) = 0 \tag{1}$$

$$\rho(u.\nabla u) = -\nabla p + \nabla.\{\mu\{\nabla u + (\nabla u)^{Tr}\} - \mu_t\{\nabla u + (\nabla u)^{Tr}\}\} \tag{2}$$

$$\rho C_p u.\nabla T = \nabla.\{(k + \frac{C_p \mu_t}{Pr_t})\nabla T \tag{3}$$

$$Q = \nabla.(k_s)\nabla T \tag{4}$$

Heat transfer from the solid wall is passed on to the adjoining fluid walls, with the use of coupling boundary condition. This condition equates the heat flux from the solid to heat flux in the fluid region.

$$k_s \frac{\partial T}{\partial y} = k \frac{\partial T}{\partial y} \tag{5}$$

$$T_s = T \text{ (At wall)} \tag{6}$$

Boundary condition for heated bottom wall is

$$q = k_s \frac{\partial T}{\partial y} \tag{7}$$

Adiabatic wall boundary condition is imposed on other non-fluid surfaces.

3.2 Computational domain and mesh details

The computational domain used in this study to model the baseline PFHS is shown in Fig.3. Only one channel with two adjoining plate fins are used to model the PFHS. The outer side of plate fins are assigned with symmetry boundary condition, and the modelled plate fin's thickness is half of the actual plate fin's thickness. Flow velocity is specified at the inlet, and top and bottom side of fluid domain are specified with zero shear walls. Zero static pressure is specified at the channel outlet. Side surfaces are specified with symmetry boundary condition and at the bottom of the solid heat sink, specified heat power value of 10W is imposed.

The mesh for the computational domain is generated in Ansys. The solid domain is discretized with tetrahedral cells while the fluid domain is discretized with prismatic cells near the wall followed by tetrahedral cells (Fig.4). 14 layers of prismatic cells are maintained to resolve the high gradient boundary layer flow accurately. The total mesh size for baseline PFHS is 5.77Million cells and the mesh size for PFHS with the VG is 6.44 million cells. The simulation was considered to have converged when the change in temperature over the last 100 iterations is less than 0.01K and the mass flow imbalance is less than $1x10^{-7}$ kg/s.

A grid independence study is carried out to estimate the mesh error and the results are shown in (Fig.4). The CFD simulations are carried out on three different meshes of size 2.66million, 6.44million and 14.30million, to compute the grid convergence index [32] on Nu and friction factor. Both Nu and friction factor have shown monotonicity with the mesh refinement. The error due to mesh on Nu of 6.44million mesh is 0.18%, while the same error on 14.30million mesh is 0.03%. Since the error on 6.44millions mesh is <1% and it can considerably reduce the computational cost, this mesh is chosen for further study. For the selected mesh, the error on friction factor is found to be 0.250%.

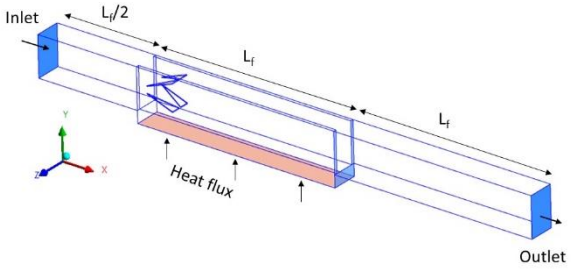


Fig. 3. Computational domain used for the heat sink study

To evaluate and rank the various PFHS configuration with VG, the heat transfer coefficient (HTC), Nu, friction factor, and THP parameter (Eq. (8-12)) were evaluated. The expression for the THP is based on the constraint of identical pumping power between different flow simulations. Mass weighted averaging was used to calculate the temperature at the inlet (T_{in}) and outlet (T_{out}). D_h is the hydraulic diameter of the channel and L_f is the length of heat sink channel. T_w is the area averaged bottom wall temperature and A_{HT} is the total area of heat transfer sur-

faces. To calculate Nu, the PFHS channel's length and air's thermal conductivity are used as references. THP is calculated by using the performance parameters of baseline PFHS (Nu_s, f_s) and PFHS with VG (Nu, f).

$$T_{ave} = \frac{(T_{out} + T_{in})}{2} \quad (8)$$

$$HTC = \frac{\dot{m}Cp(T_{out} - T_{in})}{A_{HT}(T_w - T_{ave})} \quad (9)$$

$$Nu = \frac{HTC.L_f}{k} \quad (10)$$

$$f = \frac{2.\Delta P}{\rho u^2}\left(\frac{D_h}{L_f}\right) \quad (11)$$

$$THP = \frac{Nu/Nu_s}{(\frac{f}{fs})^{1/3}} \quad (12)$$

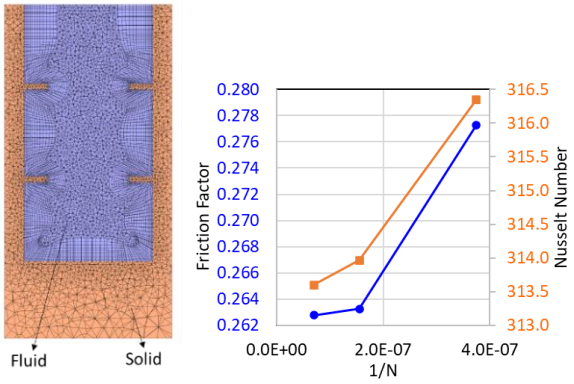


Fig. 4. a) Mesh details and b) Grid independence study results

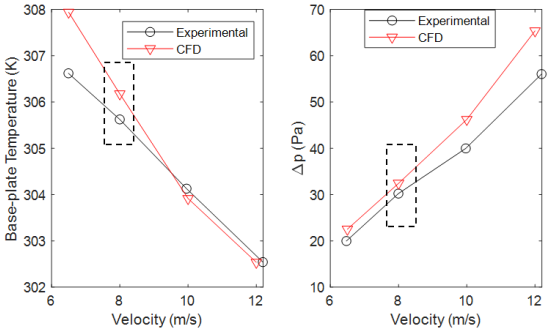


Fig. 5. Validation of CFD modelling by comparing against the experimental data of [29]

In this study, characteristics of PFHS with VG are evaluated at 8m/s velocity, so the CFD error at 8m/s velocity is highlighted here. This velocity is chosen because the heat sink channel flow is created by mini fans and the air velocity generated by them varies from 2 to 8m/s. As this work intends to evaluate higher heat transfer achievable by fan and heat sink, it is decided to evaluate the heat sink performance at higher air velocity, hence 8m/s is chosen. Since cooling fans don't produce velocities above 8m/s, higher flow velocities are not considered for this study. The numerical setup of this study was validated by comparing against the results of [29] (Fig. 5). Jonsson and Moshfegh [29] conducted wind tunnel test to evaluate the performance of heat sinks with 7 different fin types (including plate fins) in the Re range of 2000 to 16500. Electrical circuit with a heat load of 10W is used to heat the heat sinks. Temperatures are measured with type T thermocouples while pressures are measured with Autotran 700D pressure transducers after the conditions attain steady state. Volumetric air flow is measured using a laminar flow element. Based on the test results they developed correlations to predict Nu and dimensionless pressure drop. The experimental uncertainty reported by [29] on Δp measurement is ±0.61% (min) to ±30.4% (max) and the uncertainty on mean velocity is ±2.26%(min) and ±3.39% (max). It was reported that the large error (max) limits in pressure drop are due to the inaccuracy in measuring small pressure drops (Pressure drop smaller than 0.5Pa have been discarded in the measurement). The specified accuracy of thermocouples used for temperature measurement is ±0.5°C. The validation of this CFD study shows that at 8m/s velocity, the difference between pressure predicted by CFD and the experiment is 7.3%, while the difference in baseplate temperature is 0.2%.

3.3 Response Surface Model details

To evaluate the heat transfer characteristics of single and multiple pairs of VG on vertical fins, three design parameters namely, Height(H), Length(L), and axial distance between two consecutive VG pairs (Δx) are considered (Fig.2). The authors have conducted a study to evaluate the effect of attack angle (8 to 30deg) and found that high attack angles are required for better THP [28]. Hence in this study, VGs are fixed at a constant attack angle (β) of 20°. The gap between the leading edges of a winglet pair (g) is 0.0015m. The leading edge of first pair of VG is fixed at 0.002m (xloc) from the plate fin's leading edge.

After evaluating the performance of different number of VG pairs on the vertical fin, response surface models for Nu and THP were generated in terms of the design parameters for the PFHS with DPVG. A CFD based, 15 point, design of experiment has been conducted for the DPVG configuration based on Box-Behnken design. Box-Behnken design is chosen as it is desired to keep the number of experiments required for the model development within an acceptable limit. The design parameters bound for the three design variables, are shown in Table 2. VG height (H) is non-dimensionalised with width of the channel (W_c) and it was allowed to vary from 0.2 to 0.45. VG length is non-dimensionalised with respect to height of the VG and the maximum length is limited to 5.2 times of the VG height. Axial distance between leading edges of consecutive VG pairs is nondimensionalized with respect to the length of the plate fin, and it is allowed to take a maximum value of 0.75. The thickness of the delta winglet is considered as $2x10^{-4}$m.

	Minimum	Maximum	Mean
H/W_c	0.2	0.45	0.325

L/H	1	5.2	3.1
$\Delta x/L_f$	0.30	0.75	0.525

Table 2. Design variable limits for PFHS with DPVG on vertical fins.

4. Results and Discussion

In this study, performance of SPVG mounted on vertical fins of PFHS is compared against PFHS with DPVG and TPVG. Based on the comparison, PFHS with DPVG are chosen for further studies.

4.1 Effect of multiple pairs of VG on PFHS

In order to assess the effect of VG, CFD simulation of PFHS without VG, with SPVG, DPVG and TPVG are separately conducted, and the thermal performance parameters are evaluated (Table 3). The delta winglet VG pairs are mounted in CFDN arrangement on the vertical plate fins. The geometric parameters of delta winglet VG are H/Wc= 0.45, and L/H=1.378. The inter-VG distance in DPVG and TPVG are kept the same ($\Delta x/L_f$=0.309). Velocity and temperature field (Fig.6, Fig.7) of PFHS with different number of VG pairs, show that the presence of a VG, increases the mixing of cold air with hot air within the channel. Heat transfer increment by the VG can be explained through field synergy principle. Reference [33] postulated that by aligning the local flow velocity with the heat flux vector or temperature gradient vector, convective heat transfer from a given surface can be increased. In PFHS, VGs generate a secondary flow (swirling flow) and this flow vector is aligned with the heat flux vector, hence the heat transfer increases. Presence of an additional pair of VG, increases the flow velocity within the channel (compare Fig.6 (b) and (d)) and also enhances the secondary flow and mixing of the fluid within the heatsink channel. This leads to further increase in heat transfer performance of PFHS, and it is evident by the reduction of plate fins wall temperature as shown in Fig.7.

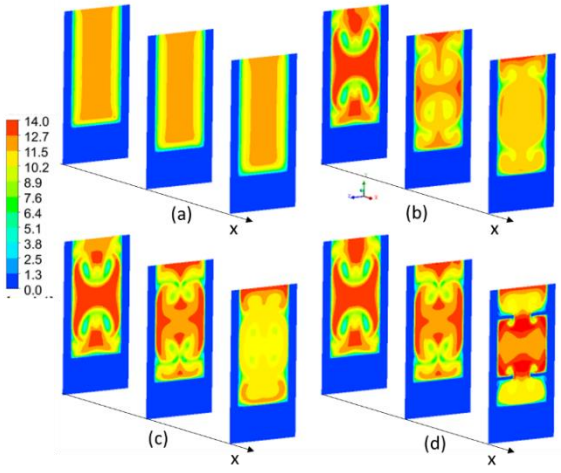


Fig. 6. Velocity (m/s) field at different axial stations on a) PFHS, b)PFHS with SPVG, c) PFHS with DPVG and d)PFHS with TPVG

Configuration	Nu	Friction Factor	THP
No VG	172.65	0.1082	1.000
SPVG	263.94	0.2010	1.2437
DPVG	313.97	0.2648	1.3496
TPVG	356.32	0.3300	1.4233

Table 3. Performance of PFHS without VG, and with different number of pairs of VG

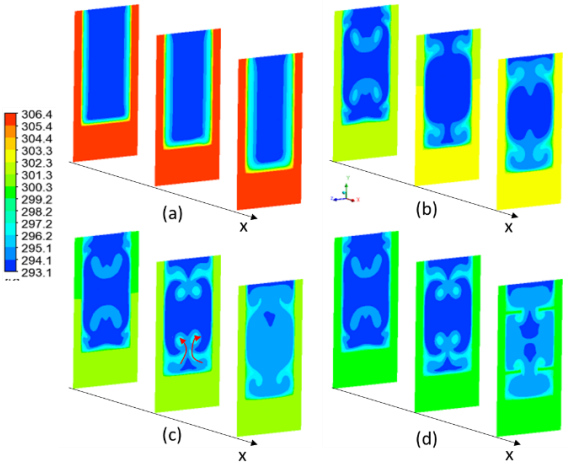


Fig. 7. Temperature (K) field at different axial stations on a) PFHS, b) PFHS with SPVG, c) PFHS with DPVG and d) PFHS with TPVG

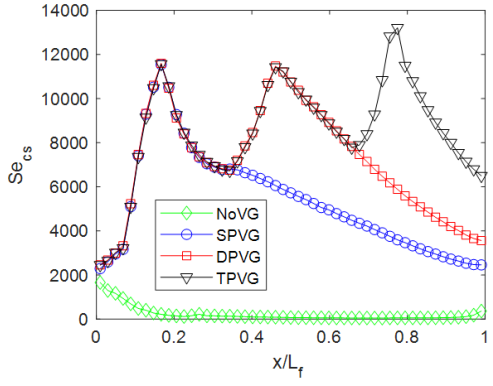


Fig. 8. Secondary flow intensity distribution on PFHS with no-VG, SPVG, DPVG and TPVG

The intensity of the secondary flow created by the VG can be calculated using a non-dimensional number (Se) defined by Song and Wang[34] (Eq.13). High value of Se results in high levels of heat transfer and Nu.

$$Se = \frac{\rho D_h^2}{\mu}\left(\frac{\int_\Omega |\omega_n| d\Omega}{\int_\Omega d\Omega}\right) \quad (13)$$

$$Se_{cs} = \frac{\rho D_h^2}{\mu}\left(\frac{\int_A |\omega_n| d\mathrm{ydz}}{\int_A d\mathrm{ydz}}\right) \quad (14)$$

To calculate the axial variation of secondary flow intensity,

cross-sectional area averaged Se, denoted as Se_{cs}, can be calculated using Eq.14. The variation of Se_{cs} along the heat sink channel length shows (Fig-8) that at the VG location secondary flow intensity reaches maximum and this gradually decreases in the downstream direction. The figure shows that effectiveness of third VG pair could not be fully utilized in this PFHS, as its location is quite close to the trailing edge of the channel.

The Nu and THP are calculated for PFHS with different number of VG pairs (Table 3, Fig.9). The PFHS performance against the number of VG pairs show that, though the performance improves due to an additional VG pair, the performance improvement rate decreases with increase in number of VG pairs on the vertical fin. The THP of DPVG is 8.5% higher than the THP of SPVG, while the THP of TP VG is only 5.5% higher than the DPVG. Every additional VG pair increases the secondary flow by the same amount, but at aft location, the fluid is already warm and the net difference in temperature between wall and fluid decreases. So, the possible amount of heat transfer is low. Further the third VG pair's location is so aft that there is not enough length of the heat sink plates available to utilize the VG effect. Hence, the authors feel that evaluating the characteristics of DPVG on PFHS will be more useful to the heat sink designers than the characteristics of TPVG on PFHS.

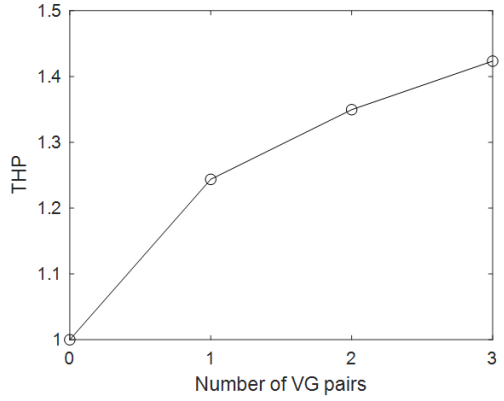


Fig. 9. Variation of THP with respect to number of VG pairs

4.2 Response Surface Model for PFHS with DPVG

A fifteen-point DoE based on Box-Behnkin type sampling is carried out to evaluate the effect of design variables (H, L, Δx) on the performance of PFHS with DPVG. Based on the CFD results, Nu, friction factor and THP parameters are evaluated. A polynomial response surface model (Eq. (15)) for the Nu and THP are developed which have linear, quadratic and interaction terms between the design variables. It should be noted that all the design variables are scaled to similar magnitude of range [-1,1] before the response surface model was developed. The variables H, L and Δx represent height, length and axial distance between VG pairs respectively and the coefficient values of model equation are given in Table 4. R^2 statistic is a measure of how close the data are to the fitted regression line and is calculated based on Eq.(16). In this equation $\boldsymbol{y_i}$ denotes the response variable (Nu) and $\boldsymbol{f_i}$ denotes the response value predicted by the fit and $\bar{\boldsymbol{y}}$ is the mean of all response variables. $\boldsymbol{R^2}$ value for Nu and THP model are 94.8% and 90.5% respectively, which indicates that the response models have good accuracy.

$$Y = \alpha_0 + \alpha_1 H + \alpha_2 L + \alpha_3 \Delta x + \alpha_4 H^2 + \alpha_5 L^2 + \alpha_6 (\Delta x)^2 + \alpha_7 HL + \alpha_8 L\Delta x + \alpha_9 H\Delta x \quad (15)$$

$$R^2 = 1 - \frac{\sum_i (y_i - f_i)^2}{\sum_i (y_i - \bar{y})^2} \quad (16)$$

	Nu	THP		Nu	THP
α_o	255.264	1.2390	α_6	-16.340	-0.0567
α_1	42.006	0.0639	α_7	26.128	0.0415
α_2	39.503	0.1108	α_8	-2.424	-0.0114
α_3	-15.670	-0.0692	α_9	-20.772	-0.0885
α_4	-2.932	-0.0614	R^2 statistic	94.80	90.51
α_5	3.866	0.0132			

Table 4. Coefficient values of model equation corresponding to Nu and THP of PFHS with DPVG

From Fig.10 and 11 it could be observed that Nu prefers higher VG height but THP prefers medium height to keep the friction factor penalty low. The THP model (Fig.11) indicates that VG's length is a strong design parameter than its Height. As the inter VG distance increases the THP performance decreases. VG Length is mostly a linear variable with a weak quadratic behaviour. It is also noted that the cross interaction between L and Δx is the weakest while the cross interaction between H and Δx is the strongest among the other interactions.

4.3 Effect of axial inter-VG distance

The response surface model indicates that for better heat transfer performance the inter-VG distance (Δx) should be less. To understand the physics, PFHS with DPVG with inter-VG distances of 1L, 2.25L, 3.05L and 3.86L are modelled (L- Winglet length) and their performance are evaluated using CFD.

Inter-VG axial distance		Nu	Friction Factor	THP
Δx/L	$\Delta x/L_f$			

1.00	0.137	310.20	0.2578	1.3453
2.25	0.309	313.97	0.2648	1.3496
3.05	0.418	313.65	0.2657	1.3467
3.86	0.527	309.92	0.2656	1.3309

Table 5. Effect of inter-VG distance on PFHS with DPVG

Results (Table 5) show that fixing the second VG pair at an inter-VG distance of 2.25L yields higher THP and Nu than fixing at other Δx values. Fixing the second VG immediately after the first VG (Δx=1L) did not yield maximum heat

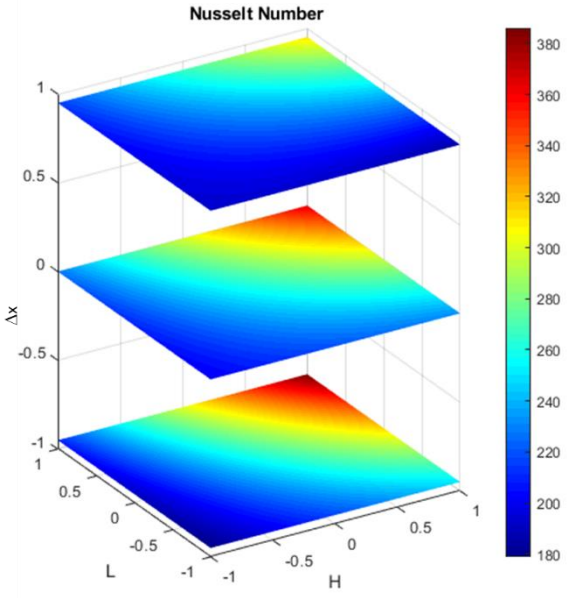


Fig. 10. Variation of Nu with respect to different design variables for PFHS with DPVG

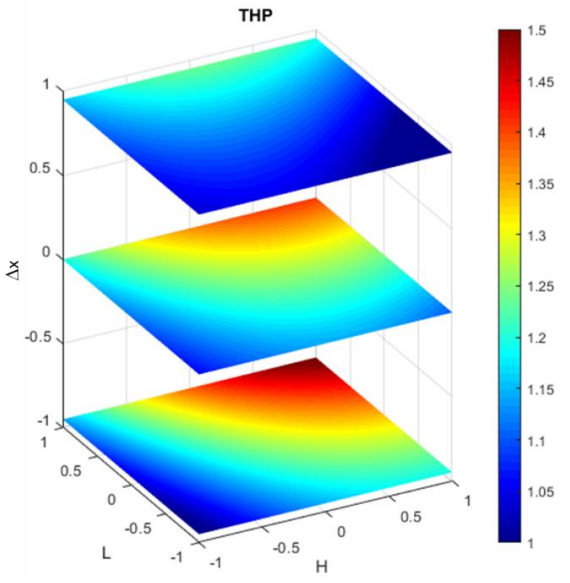


Fig. 11. Variation of THP with respect to different design variables for PFHS with DPVG

transfer performance. For optimum performance, suitable amount of gap must be present between the first VG pair and the second VG pair. An inter-VG distance of 2.25L to 3.05L gives good heat transfer performance.

Axial variation of mass flow averaged fluid temperature and bottom plate's mid-line temperature are shown in Fig.12. Inter-VG distance of 2.25L, leads to good heat transfer hence it has higher fluid temperature than Δx=3.05L and 3.86L cases. Inter VG distance of 3.86L, leads to comparatively higher bottom wall temperature at the leading edge and this relates well with the lower performance of this case. Δx=2.25L results in higher bottom wall temperature at the aft end, but Fig-13 (b) shows that this case has lower vertical plate temperature near the leading edge. Hence overall, Δx=2.25L case results in best performance.

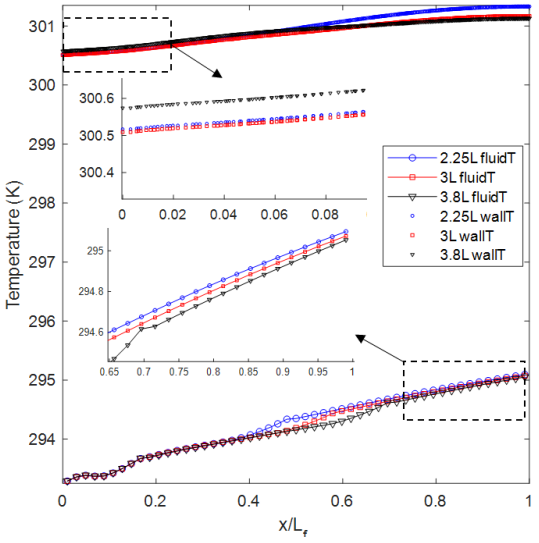


Fig. 12. Axial variation of fluid temperature and bottom wall temperature for different inter-VG distance

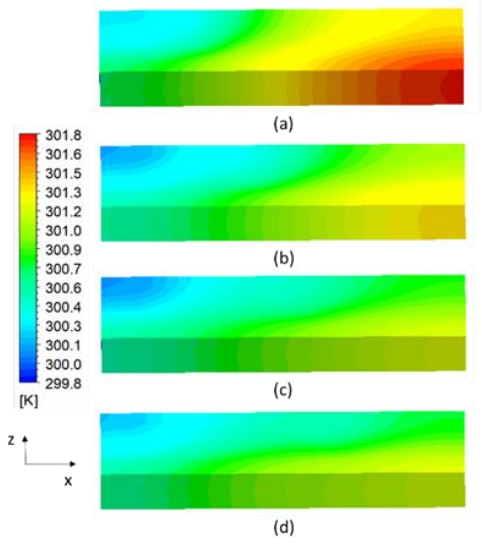


Fig. 13. Temperature field (K) on the PFHS with DPVG with Δx values of a) 1L, b) 2.25L, c) 3.05L and c) 3.86L

Temperature distribution (Fig.13) on the vertical fin and bottom plate shows that Δx=2.25L and 3.05L keep the forward part (and to reasonable extent rear part) of vertical fin cooler while Δx=3.86L not able to keep the forward part cooler but keeps only the rear part cooler. Hence overall, 2.25L and 3.05L inter-VG distances yield better performance than 3.86L distance. The inter-VG distance of 3.86L, is quite large that, at the second VG location flow is already warmer due to heat transfer of upstream part. So, in spite of high secondary flow generation by VG (Fig 14), due to reduced (Tw-Tf), the heat transfer augmentation is low. Further, for maximum benefit from DPVG, the secondary flow of both the VG pairs should be available for sufficient downstream length of the heatsink. At the same time, second VG should not be placed immediately after the first VG, but an inter-VG distance of 2L to 3L is desirable.

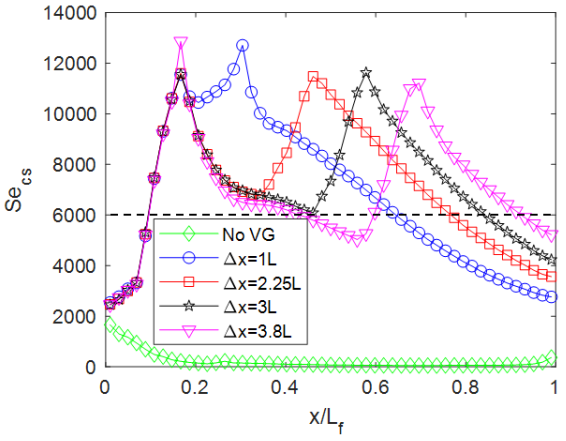


Fig. 14. Secondary flow intensity factor distribution for different inter VG distances

4.4 Effect of DPVG on the heat transfer efficiency of PFHS

Heat exchanger efficiency is defined as the ratio of the heat transferred in the actual heat exchanger to the heat that would be transferred in the ideal heat exchanger [35]. In general, efficiency provides a clear and quantitative measure of the given systems performance relative to ideal systems performance. In this study heat exchanger efficiency of baseline PFHS and PFHS with best performing DPVG are evaluated using the below formulas Eq. (17-19).

$$\eta = \frac{Q_{actual}}{Q_{max}} \quad (17)$$

$$Q_{actual} = -k_s A_c \frac{\partial T}{\partial y}|_{y=0} \quad (18)$$

$$Q_{max} = HTC.A_{HT}(T_w - T_{in}) \quad (19)$$

Actual heat transfer is calculated in terms of conductive heat transfer taking place from the heat flux boundary. Assuming radiative heat transfer is zero, conduction will be equal to convective heat transfer in this study. A_c represents cross sectional area of the plate fins. Temperature gradient is calculated at 11 different axial stations on the PFHS and a mean value is used for Q_{actual} calculation. To calculate the Q_{max}, averaged HTC and averaged temperature of the base-plate are used. The efficiency results at the flow velocity of 8m/s (Table-6) show that, presence of DPVG increases the heat transfer efficiency by 24.8% compared to baseline PFHS. This efficiency improvement agrees well with other theories (eg. field synergy principle) which has shown that VG will enhance the heat transfer due to secondary flow generation.

	Q_{actual} (W)	Q_{max} (W)	Efficiency (%)
No VG	0.4276	0.7752	55.16
DPVG	0.4242	0.5303	79.99

Table 6. Heat exchanger efficiency of PFHS with no VG and PFHS with DPVG

4.5 Performance of PFHS with DPVG relative to velocity

In order to calculate the change in performance of PFHS with DPVG relative to velocity, the best-performing PFHS with DPVG configuration is evaluated at different inlet velocities. The variation of Nu and THP with respect to velocity is given in Fig.15. Nu increases as the velocity increases, but the friction factor and THP decreases as the velocity increases. Ratio of Nu of PFHS with DPVG to Nu of baseline (Nu/Nu_s) decreases with velocity, so the THP, which is proportional to this ratio is also decreases with velocity. This shows that VGs are thermally more effective at low velocities than at high velocities.

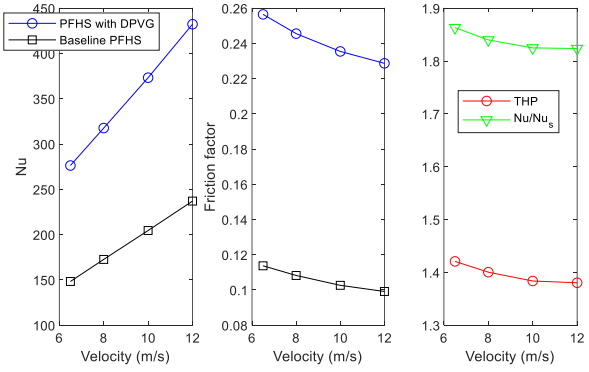


Fig. 15. Variation of Nu and THP with respect to velocity for PFHS with DPVG

5. Conclusions

In this study heat transfer characteristics of different number of VG winglet pairs mounted on the vertical fins of PFHS is evaluated computationally. The delta winglet pair VGs are fixed in CFDN arrangement. The CFD methodol-

ogy is validated by comparing against the available literature [29] experimental results. Based on the CFD results, the effect of each of the design parameters of VG pairs were evaluated, and a polynomial response surface model was developed for the Nu and THP of PFHS with DPVG. Further the ideal inter-VG distance and the variation of PFHS with VG performance relative to velocity were also evaluated. The results show that,

- As the number of VG pairs on the PFHS increases, the heat transfer performance increases but the performance increment rate decreases. The THP of PFHS with DPVG is 8.5% higher than the THP of PFHS with SPVG, while the THP of TPVG is only 5.5% higher than the DPVG.
- Double pair of delta winglet VG with ideal design parameter values can improve the THP of PFHS by 49%.
- Response surface model generated based on DoE indicates that the VG length is a more critical design parameter than the VG height, with respect to THP performance. To achieve maximum heat transfer performance from the DPVG, the inter-VG distance must be around 2.2 to 3.0 times the length of delta winglet.
- With increase in velocity, the THP of PFHS with DPVG decreases because the heat transfer increment due to VG is not sufficiently higher than the heat transfer increment due to flow velocity. So VGs are more effective at lower velocities than at higher velocities.

Acknowledgements

The author wants to thank Dr. Krishnan A. S., Associate professor, Coimbatore Institute of Technology for the valuable discussions on heat exchangers. The author also thanks the anonymous reviewers for their insightful comments.

Nomenclature

A_{HT}	: Total area of heat transfer surface(m^2)
A_c	: Cross sectional area of plate fins (m^2)
CFDN	: Common Flow Down
CFU	: Common Flow Up
Cp	: Specific heat capacity at constant pressure (J/kg/K)
D_h	: Hydraulic diameter of PFHS channel (m)
DoE	: Design of Experiments
ΔP	: Pressure difference between inlet and outlet (Pa)
DPVG	: Double pair of vortex generators
Δx	: Axial distance between the consecutive VG pairs (m)
f	: Friction factor
g	: Gap between winglet pair on the vertical plate (m)
H	: Height of delta winglet (m)
H_f	: Height of fin (m)
HTC	: Heat Transfer Coefficient
k	: Thermal conductivity of fluid (W/m/K)
ks	: Thermal conductivity of solid (W/m/K)
L	: Length of delta winglet (m)
Nu	: Nusselt Number
Nu_s, f_s	: Nu and f of baseline PFHS
p	: Fluid pressure (Pa)
PFHS	: Plate fin heat sink
Pr	: Prandtl number
q	: Heat flux (W/m^2)
ρ	: Density (kg/m^3)
Re	: Reynolds number
Se	: Secondary flow intensity factor
SPVG	: Single pair of vortex generators
THP	: Thermal Hydraulic Performance
Tin	: Inlet Temperature (K)
Tout	: Outlet Temperature (K)
TPVG	: Triple pair of vortex generators
Tw	: Averaged base plate temperature (K)
u	: Flow velocity (m/s)
VG	: Vortex Generators
Wc	: Channel width (m)
$\dot{m}$	: Mass flow rate (kg/s)
μ	: Dynamic viscosity (Nsm^{-2})
β	: Winglet attack angle (deg)
α	: Coefficients of response surface model
δ	: Plate fin thickness (m)
ω_n	: Vorticity in the normal direction of cross section (1/s)

References

[1] M. Fiebig, P. Kallweit, N. Mitra, S. Tiggelbeck, Heat transfer enhancement and drag by longitudinal vortex generators in channel flow, *Experimental thermal and fluid science*, 4 (1) (1991)

[2] S.M. Pesteei, P.M.V. Subbarao, R.S. Agarwal, Experimental study of the effect of winglet location on heat transfer enhancement and pressure drop in fin-tube heat exchangers, *Appl. Therm. Eng.* 25 (11-12) (2005) 1684-1696.

[3] J.M. Wu, W.Q. Tao, Numerical study on laminar convection heat transfer in a rectangular channel with longitudinal vortex generator. Part B, parametric study of major influence factors, *Int. J. Heat Mass Transfer* 51 (13-14), (2008), 3683-3692.

[4] K. Yang, J. Jhong, Y. Lin, K. Chien, C. Wang, On the

heat transfer characteristics of heat sinks: with and without vortex generators, *IEEE trans. Components and packaging technologies*, 33, (2), (2010)

[5] J.M. Wu, W.Q. Tao, Effect of longitudinal vortex generator on heat transfer in rectangular channels, *Applied therm. Engg.*, 37, (2012), 67-72.

[6] H. Y. Li, C. Chen, S. Chao, G. Liang, Enhancing heat transfer in a plate fin heat sink using delta winglet vortex generators, *Int. J. Heat Mass Transfer*, 67, (2013), 666-677.

[7] H.Y. Li, W. Liao, T. Li, Y. Chang, Application of vortex generators to heat transfer enhancement of a pin-fin heat sink*, Int. J. Heat Mass transf.*, 112 (2017) 940–949.

[8] Y.-L. He, P. Chu, W-Q. Tao, Y-W. Zhang, T. Xie, Analysis of heat transfer and pressure drop for fin-and-tube heat exchangers with rectangular winglet-type vortex generators, *Appl. Therm. Eng.,* 61, (2) (2013) 770–783.

[9] A. Sinha, H. Chattopadhyay, A. K. Iyengar, G. Biswas, Enhancement of heat transfer in a fin-tube heat exchanger using rectangular winglet type vortex generators*, Int. J. Heat Mass Transf.*, 101 (2016) 667–681.

[10] A. Sinha, K.A. Raman, H. Chattopadhyay, G. Biswas, Effect of different orientations of winglet arrays on the performance of plate-fin heat exchangers, *Int. J. of Heat and Mass transfer,* 57, (2013), 202-214.

[11] G. Zhou, Experimental investigations of heat transfer enhancement by plane and curved winglet type vortex generators with punched holes, *I. J. of Thermal sciences,* 78, (2014), 26-35.

[12] M.K. Aliabadi, S. Zangouei, F. Hormozi, Performance of a plate-fin heat exchanger with vortex-generator channels: 3D-CFD simulation and experimental validation*, I. J. of Thermal sciences*, 88, (2015), 180-192.

[13] M. K. Aliabadi, O. Sartipzadeh, A. Alizadeh, An experimental study on vortex-generator insert with different arrangements of delta-winglets, *Energy,* 82, (2015) 629–639.

[14] A. Datta, A. Das, P. Dey and D. Sanyal, Multi objective optimization of laminar heat transfer and friction factor in rectangular microchannel with rectangular vortex generators: An application of NSGA II with gene expression programming metamodel, *Journal of Heat transfer*, 139, (2017).

[15] A. Abdollahi, M. Shams, Optimization of shape and angle of attack of winglet vortex generator in a rectangular channel for heat transfer enhancement, *Appl. Therm. Eng.*, 81 (2015) 376–387.

[16] M. Samadifar, D. Toghraie, Numerical simulation of heat transfer enhancement in a plate-fin heat exchanger using a new type of vortex generators, *Appl. Therm. Eng.,* 133 (2018) 671–681.

[17] A. Akcayoglu, C. Nazli, A comprehensive numerical study on thermohydraulic performance of fluid flow in triangular ducts with delta-winglet vortex generators, *Heat transfer engineering*, 39,(2), (2018),107-119.

[18] H.E. Ahmed, Optimization of thermal design of ribbed flat-plate fin heat sink, *Applied Thermal Engg.*, 102 (2016), 1422-1432.

[19] H. Liu, C. Fan, Y. He, D.S. Nobes, Heat transfer and flow characteristics in a rectangular channel with combined delta winglet inserts*, Int. J of Heat and Mass transfer,* 134, (2019), 149-165.

[20] K. Song, T. Tagawa, Z. Chen, Q. Zhang, Heat transfer characteristics of concave and convex curved vortex generators in the channel of plate heat exchanger under laminar flow*, Int. J of Thermal sciences*, 137, (2019), 215-228.

[21] H. Naik, S. Tiwari, Effect of winglet location on performance of fin-tube heat exchangers with inline tube arrangement, *Int. J. of Heat and Mass transfer,* 125, (2018), 248-261.

[22] H. Naik, S. Harikrishnan, S. Tiwari, Numerical investigations on heat transfer characteristics of curved rectangular winglet placed in a channel*, Int. J of Thermal Sciences,* 129, (2018), 489-503.

[23] M. Awais, A. Bhuiyan, Enhancement of thermal and hydraulic performance of compact finned-tube heat exchanger using vortex generators (VGs): A parametric study, *Int. J of Thermal Sciences,* 140, (2019), 154-166.

[24] H.E. Ahmed, H.A. Mohammed, M.Z. Yusoff, An overview on heat transfer augmentation using vortex generator and nano fluids : Approaches and applications, *Renewable and sustainable energy reviews*, 16 (2012), 5951-5993.

[25] N. Zheng, F Yan, K. Zhang, T. Zhou, Z. Sun, A review on single-phase convective heat transfer enhancement based on multi-longitudinal vortices in heat exchanger tubes, *Applied Therm. Engg.*, 164, (2020),114475.

[26] D.P. Sam Solomon, V. Selladurai, A.S. Krishnan, Experimental analysis on performance assessment of a hybrid double cross flow tube arrangement in a shell and tube heat exchanger. *Journal of Mechanical Science and Technology,* 36 (1), (2022), pp.499-511.

[27] M. Santhanakrishnan, T.Tilford, C.Bailey, Multi-objective NSGA-II based shape optimisation of the cross-sectional shape of the passively cooled heat sinks*, Int. J. of Numerical methods for Heat and fluid flow*, 32, (3), (2022) pp.1025-1045.

[28] M. Santhanakrishnan, T.Tilford, C.Bailey, Heat transfer characteristics of plate fin heat sink with longitudinal vortex generators, *Int. J. of Numerical methods for Heat and fluid flow,* 33 (3), (2023), pp.1203-1228.

[29] H. Jonsson and B. Moshfegh, Modeling of the thermal and hydraulic performance of plate fin, strip fin and pin fin heat sinks – Influence of flow bypass, *IEEE transactions on components and packaging technologies*, 24, (2), (2001).

[30] F. Zhou and I Catton, Numerical evaluation of flow and heat transfer in plate-pin fin heat sinks with various pin

cross-sections, *Numerical Heat transfer, Part A Applications*, 60, (2011) 107-128.
[31] Menter, F. R., Zonal Two Equation k-ω Turbulence Models for Aerodynamic Flows, *AIAA Paper* 93-2906 (1993).
[32] P.J. Roache, Quantification of uncertainty in computational fluid dynamics, *Annual. Rev. Fluid Mech*. 29 (1) (1997) 123–160.
[33] J.M. Wu, and W.Q. Tao, Numerical study on laminar convection heat transfer in a rectangular channel with longitudinal vortex generator. Part A: Verification of field synergy principle, *Int. J. of Heat Mass Transfer*, 51 (5-6), (2008), pp.1179-1191.
[34] K. Song, L.B. Wang, The effectiveness of secondary flow produced by vortex generators mounted on both surfaces of the fin to enhance heat transfer in a flat tube bank fin heat exchanger, *J. Heat Transfer*, 135 (4), (2013)
[35] A. Fakheri, Heat exchanger efficiency, *J. Heat Transfer*, 129(9), (2007), pp.1268-1276.

Author information



Mani S. Santhanakrishnan received the B.Tech. degree in Aeronautical Engineering from Madras Institute of Technology, Chennai and the M.Eng. degree in Aerospace Engineering from Indian Institute of Science, Bangalore, India. He has worked in aerospace industry for 12 years on various capacities. He has completed PhD in the field of Topology Optimization at the University of Greenwich, United Kingdom in 2018 and currently working as a research fellow in the Cranfield University, UK. He has authored 2 patents, 9 conference papers and 4 journal articles. His research interests are Engineering optimization, Heat transfer, Aerodynamics, CFD and Turbomachinery.



https://dspace.org/

Effect of multiple pairs of vortex generators on the thermal performance of plate fin heat sink

Santhanakrishnan, Mani Sekaran

2023-06-01
Springer
https://doi.org/10.1007/s12206-023-0542-2
Santhanakrishnan MS. (2023) Effect of multiple pairs of vortex generators on the thermal performance of plate fin heat sink. Journal of Mechanical Science and Technology, Volume 37, Issue 6, June 2023, pp. 3185-3195

Downloaded from a DSpace repository. https://dspace.org/